Atomic Electron Tomography of Thin Films

Aviram Bhalla-Levine, Kunwoo Park, Jungwon Park, Peter Ercius, Jianwei Miao

Microscopy and Microanalysis, **30** (Suppl 1), 2024, 1793–1795
https://doi.org/10.1093/mam/ozae044.888

Microscopy AND Microanalysis

Meeting-report

Atomic Electron Tomography of Thin Films

Aviram Bhalla-Levine[1,*], Kunwoo Park[2], Jungwon Park[2], Peter Ercius[3], and Jianwei Miao[1]

[1]*Department of Physics & Astronomy and California NanoSystems Institute, University of California, Los Angeles, CA, USA*
[2]*School of Chemical and Biological Engineering, Seoul National University, Seoul, South Korea*
[3]*National Center for Electron Microscopy, Molecular Foundry, Lawrence Berkeley National Laboratory, Berkeley, CA, USA*
*Corresponding author: abhallalevine@ucla.edu

In the past decade, the development of atomic electron tomography (AET) [1] has allowed for the 3D characterization of atomic positions in nanoparticle [2], monolayer [3], and needle [4] geometries. However, many technologically important systems are synthesized and utilized as thin films. Several challenges in sample preparation and data analysis have been overcome to expand the scope of AET to these systems. Polycrystalline yttrium-doped hafnium dioxide (HfO_2) was chosen as a model system, because it is technologically relevant as a high capacitance dielectric and ferroelectric.

New techniques were developed to synthesize a thin film sample suitable for tomography in a transmission electron microscope (TEM). Previous experiments with nanoparticle or monolayer samples involved the deposition or stamping of the material on a thin amorphous TEM grid. The amorphous thin film, typically 5-10 nm of silicon nitride or carbon, makes tomography more difficult by adding to the thickness of the sample and producing a background contrast. For a nanoparticle, this can be mitigated by calculating the background contrast in regions around the nanoparticle and subtracting this during the data analysis. This would not be possible for a thin film the sample would extend beyond the field of view. In a monolayer where samples are typically thinner than 1 nm, the additional 5-10 nm of amorphous support film is not a limiting factor. However, as technologically relevant thin films are typically 10 nm or thicker, the additional thickness of the amorphous support film will limit annular dark field (ADF) resolution, especially at higher tilt angles where the effective thickness of the sample may be more than doubled. To eliminate these issues of background contrast and thickness, a new procedure was developed. A HfO_2 thin film was synthesized on a sacrificial substrate. The film was then exfoliated and placed on a tomography grid via wet transfer. This tomography grid consists of a 50 nm thick silicon nitride window with 2 um diameter holes. A monolayer of graphene was also placed over the sample to reduce charging. A low magnification micrograph of this sample may be found in **Fig. 1**. With this configuration, the film is free-standing within the holes which minimizes background contrast and thickness.

With this sample, a tilt series was acquired on the TEAM 0.5 microscope at the National Center of Electron Microscopy, Molecular Foundry, Lawerence Berkeley National Laboratory. Annular dark field scanning transmission electron microscopy (ADF STEM) images were acquired from –67.5 degrees to +61 degrees, with 3 degree tilts. All micrographs were acquired at 300 kV, with a semi-convergence angle of 30 milliradians, and a step size of 30.5 pm. As is standard for AET, image registration was used to minimize the effect of drift by combining three micrographs from the same angle into a single image. Following this, Block-matching and 3D filtering was utilized for noise reduction. The precise alignment of projections is necessary for a successful tomography reconstruction. In the past, this has been accomplished by aligning the edge of a needle or the center of mass of a nanoparticle. For this thin film, the center of mass of a fiducial grain was used to align each projection. A medium magnification micrograph in **Fig. 1** shows an example grain. The contrast of this grain remained high relative to other grains at all projection angles.

The reconstruction was performed with the REal Space Iterative REconstruction (RESIRE) algorithm [5]. This algorithm was recently made capable of handling extended objects. This was essential for reconstructing the HfO_2 thin film that extends beyond field of view. Some visualizations of the reconstructed volume are presented in **Fig. 2** and **Fig. 3**. In these visualizations, it is possible to see atomic columns along various zone axes. Several grains, within the sample, with low and high angle grain boundaries, may also be differentiated. Further, the three dimensional reconstruction revealed the presence of cracks and voids in the film. These were not obvious from the projections alone.

In addition to further experiments, future work will involve improvements to the reconstruction and tracing of atomic positions within the reconstructed volume. Previous atomic tracing in AET experiments has allowed for some statistical analysis of various atomic properties in nanoparticles, monolayers, and needles. It is anticipated that atomic tracing of this reconstructed volume will reveal new insights about atomic arrangements at grain boundaries or void surfaces within the film. This may contribute to greater understanding of the robust capacitance and ferroelectric of HfO_2 thin films [6].

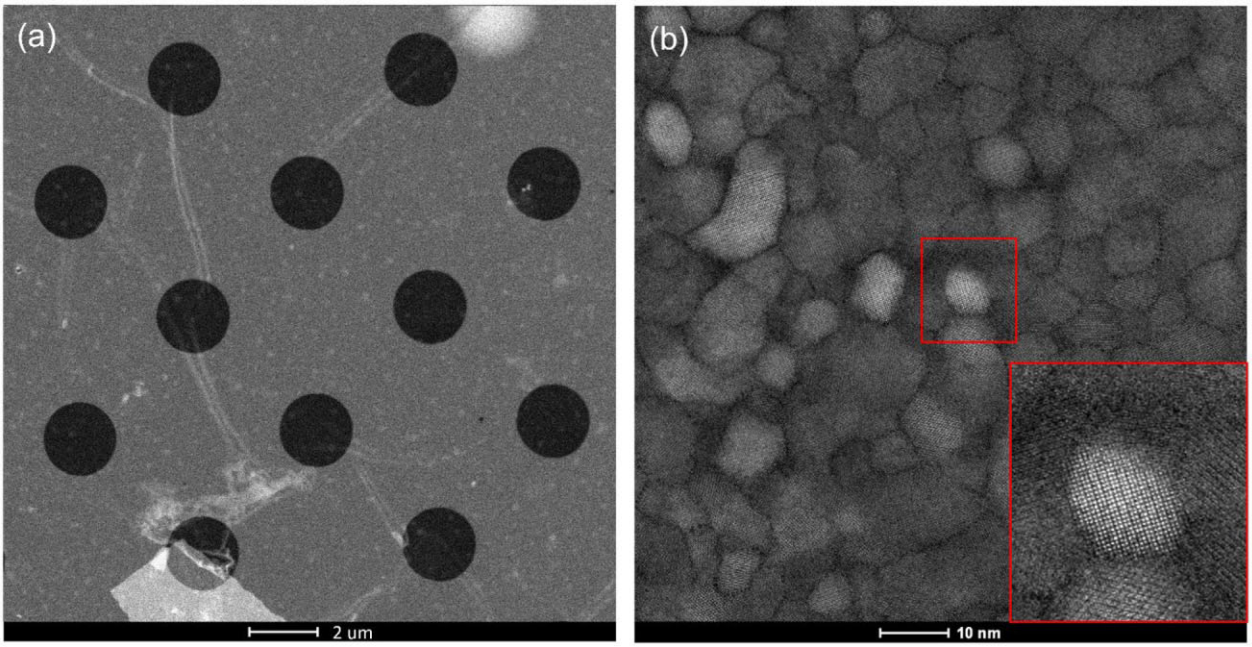

Fig. 1. (a) Low magnification ADF STEM micrograph of the HfO_2 sample. The region of bright contrast is the sample on the silicon nitride window. Within the 2 um holes, the HfO_2 film is free standing. The bright lines are folds in the monolayer graphene. (b) Medium magnification ADF STEM micrograph of the HfO_2 sample. An example fiducial marker is magnified in the red box insert.

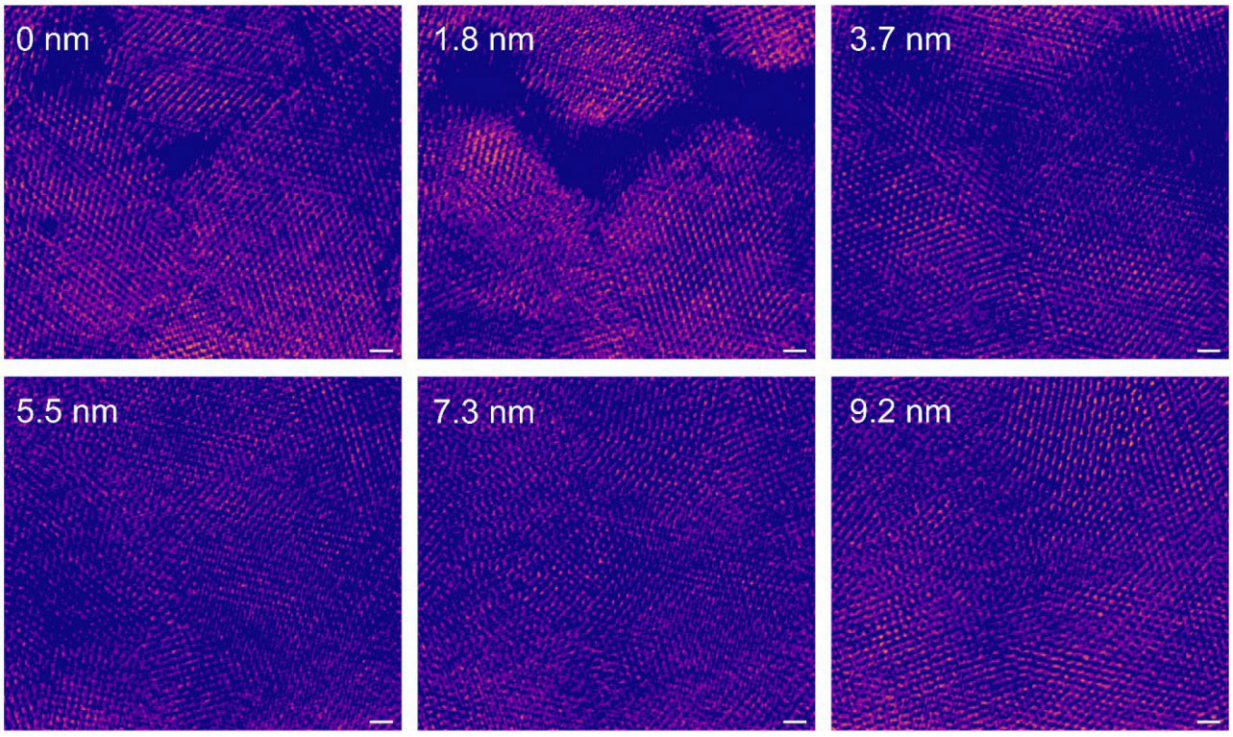

Fig. 2. 61 pm thick slices along the thickness of the film (i.e. the z direction, orthogonal to the direction of the beam at a tilt angle of zero degrees) marked by distance from the bottom of the reconstructed volume. Note the voids especially visible in the 1.8 nm slice and the high angle grain boundaries especially visible in the 9.2 nm slice. The white scale bars are 1 nm.

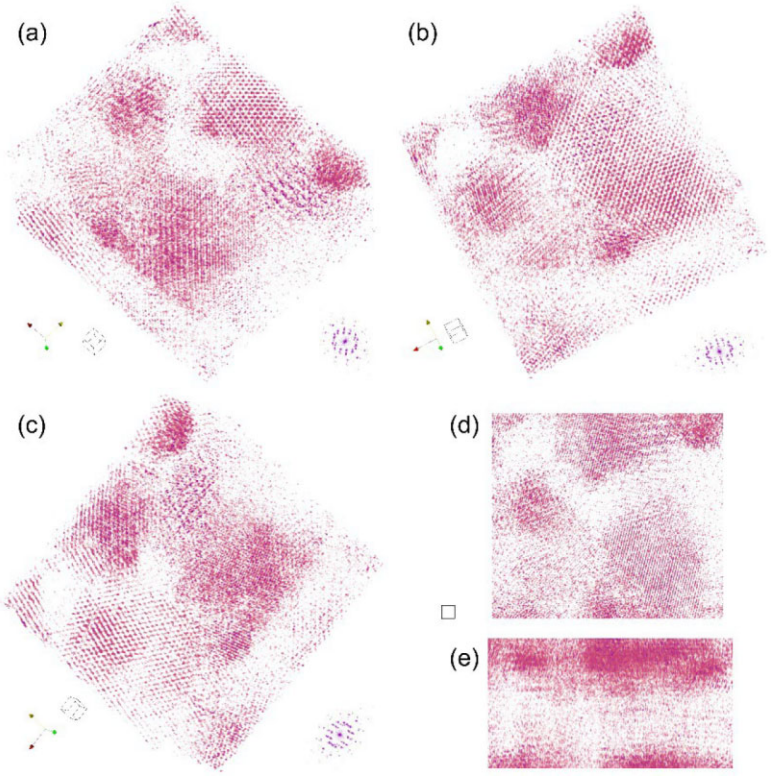

Fig. 3. (a, b, c) Volumetric representations at different angles depicting particular grains on low zone. These representations include axes indicating the orientation of the volume and a fourier transform of that volume. (d) Top view and (e) side view of the reconstructed volume. All representations include a 1 nm cube for scale.

References

1. J Miao *et al.*, *Science* **353** (2016), p. 6306. https://doi.org/10.1126/science.aaf2157
2. MC Scott *et al.*, *Nature* **483** (2012), p. 444. https://doi.org/10.1038/nature10934
3. X Tian *et al.*, *Sci. Adv.* **7** (2021), p. 38. https://doi.org/10.1126/sciadv.abi6699
4. R Xu *et al.*, *Nature Mater.* **14** (2015), p. 1099. https://doi.org/10.1038/nmat4426
5. M Pham *et al.*, *Sci. Rep.* **13** (2023), p. 5624. https://doi.org/10.1038/s41598-023-31124-7
6. The authors are grateful for the funding and resources provided from the following sources: (1) STROBE: a National Science Foundation Science and Technology Center (DMR-1548924); (2) ARO Multidisciplinary University Research Initiative program (W911NF-18-1-0431); and (3) The authors acknowledge the support from the Molecular Foundry under proposal #7867. Work at the Molecular Foundry was supported by the Office of Science, Office of Basic Energy Sciences, of the U.S. Department of Energy under Contract No. DE-AC02-05CH11231.